Journal of Engineering Science and Technology
Special Issue on Development of Sustainability Systems - III, 80 - 95

DOUBLE LAYER COIL-BASED INDUCTIVE COUPLING WIRELESS POWER TRANSFER FOR BIOMEDICAL IMPLANTS

HALA K. ABDULJALEEL[1,2,*], SADIK K. GHARGHAN[3]

[1]Electrical Engineering Department, University of Technology-Iraq, 10066 Baghdad, Iraq
[2]College of Engineering, Al-Iraqia University, Sabaa Abkar Complex, Baghdad, Iraq
[3]Middle Technical University, Electrical Engineering Technical College, Baghdad, Iraq
*Corresponding author Email: 30471@student.uotechnology.edu.iq

Abstract

Biomedical devices (BMDs) help patients' quality of life by continuously tracking their health and identifying diseases. However, BMDs' operation relies on battery power, which often has a limited lifespan. Wireless power transfer (WPT) offers an alternate solution to this specific issue. WPT technology permits the quick recharging of BMD batteries without surgical battery replacement procedures. In this paper, an inductive coupling-double layer square spiral coil (IC-DLSSC) that operated at 13.56 MHz was designed and can potentially be applied in cardiac pacemakers. The coils were fabricated using the FR4 substrate. The IC-DLSSC was examined for different parameters, such as mutual inductance, operating frequency, coupling factor, distance between transmitter and receiver coils, effect of load resistance, and transfer efficiency. The simulation and measurement results were compared to validate the performance of IC-DLSSC. The simulation transfer efficiency was 70.3% when the resistive load was 50 Ω and 10 cm transfer distance with a specific absorption rate (SAR) of 0.0689 W/kg for 1 g and 0.0108 W/kg for 10 g. While for the same distance and resistive load, the measured transfer efficiency was 59%. This study introduces an enhancement in the design of implanted devices, which leads to an acceptable transfer efficiency and SAR level to maintain patient safety in biomedical applications.

Keywords: Biomedical devices, Double layer coil, Inductive coupling, Specific absorption rate, Spiral coil.

1. Introduction

Electromagnetic waves are vital in medical and biological applications, such as diagnostic imaging and treatments, since they can pass through biological tissue [1]. Among the many waves that compose the electromagnetic field, the most penetrating are those with lower frequencies, such as microwaves and radio waves. Using the Industrial, Scientific, and Medical (ISM) band for wireless communication in medical applications allows for versatile and cost-effective remote monitoring and control of medical equipment [2]. Nevertheless, it is essential to consider safety and security considerations to safeguard patient anonymity and avert any disruption to other medical equipment. The FDA and EMA have established rules and standards for wireless communication in medical settings [3].

Electromagnetic waves transmit through tissue, increasing its temperature and causing heating. The transfer of energy is influenced by the frequency, intensity, and duration of exposure [4]. Higher frequencies have reduced tissue penetration capabilities and more concentrated heating effects, while lower frequencies can penetrate tissue deeper but less [5]. However, routine exposure to electromagnetic radiation, such as wireless communication devices or household appliances, is generally safe. The human body, consisting of 65%-70% water, allocates frequencies below 20 MHz, specifically 6.78 MHz and 13.56 MHz, for data and power transmission [6]. This is because the human body minimally dissipates energy when exposed to water. Power transmission for ISM applications uses frequencies of 6.78 MHz and 13.56 MHz, compatible with Radio Frequency Identification (RFID) standards [7].

WPT technology is promising for medical devices as it offers a secure and convenient way to power implantable devices without needing physical connectors. However, designing WPT systems requires careful consideration of power requirements, spatial separation, and safety. Devices like pacemakers, neurostimulators, and drug delivery devices use WPT technology [8]. Enhancing power transfer efficiency without compromising patient safety is possible via resonant coupling approaches, which are of the highest priority [9]. Optimal efficiency and operating range are enhanced by strategically placing several coils and maintaining a critical distance between the transmitter and receiver. Progress in Wireless Power Transfer (WPT) technology is expected to improve patient outcomes and quality of life [10].

Electronic circuits are often made using printed circuit boards (PCBs) because they are reliable and cost-effective manufacturing processes [11]. As a result of the exponential expansion of the electronics industry over the last few decades, PCB manufacture is now widely accessible and reasonably priced [12]. The surface mounting procedure and the through-hole approach are the two most prevalent methods for making printed circuit boards. PCBs offer mechanical and electrical support by linking parts such as capacitors, resistors, transformers, etc. [13]. The most common component of PCBs is glass-reinforced epoxy resin, also known as FR4. Because of their dependability and high specific strength, there are several technical uses for glass fibre-reinforced composites. Reinforcement made of silicon carbide (SiC) is popular because of its low thermal expansion, great wear resistance, and excellent thermal conductivity.

The mechanical characteristics, thermal shock resistance, and chemical erosion resistance of glass fibre were improved by adding SiC to the material [14]. PCBs may be single or double-layered, and multi-layered can be used for various purposes [15]. A single-sided PCB is the most basic kind of PCB since it consists of a single substrate (board) on which all the main electrical components are mounted, with copper traces (wires) connecting them on the other side [16]. The electrical components affixed to double-sided PCBs are linked to the substrate on both surfaces. The substrate was connected to the copper traces by bridges or vias utilizing Plated-through Hole technology. In multi-layered printed circuit boards, substrates are enclosed inside several layers, with the maximum number of layers approaching 40. The multi-layered boards are stacked and interconnected using pads or plated through holes, similar to double-sided printed circuit boards [17].

Copper is a very significant element in PCBs. Copper was a conductive layer, and the FR4 substrate was nonconductive. Copper is renowned for its malleability and ability to carry electricity [18]. Copper has exceptional tensile strength and superior thermal conductivity/expansion characteristics [19]. It has a notably lower specific electric resistivity and coefficient of thermal expansion, making it more corrosion-resistant since it has less reactivity with water than other metals. Soldering this metal is straightforward due to its ease of use [20]. The previous researchers [21, 22] achieved a good efficiency using an implanted coil with a 10 and 20 mm diameter, respectively.

Luo et al. [21] Presented a design and optimization technique for wireless power transmission in implanted brain recording micro-systems using inductive coupling coils. The method's goal is to optimize power transfer efficiency, minimize externally transmitted power, and guarantee the safety of biological tissue. Planar spiral coils are created explicitly for brain recording implants because of size constraints, transmission high-power needs, and bio-compatibility. The design functions at a frequency of 13.56 MHz, achieving a power transfer efficiency of 70%, near the theoretical maximum of 71.9%. Xu et al. [22] Presented a new and enhanced implanted wireless power transmission mechanism. A dual-coil model was developed, and the parameters influencing gearbox efficiency were examined.

Analysed the impact of coil structure using HFSS (High-Frequency Simulator Structure) simulation and verified the optimal parameters for the coil. The system connection was successfully established, and the measurements demonstrated the correlation between load and output power. The input and output powers were 200 mW and 70 mW, respectively, at a 6 mm transmission distance, at a frequency of 13.56 MHz, and an impedance of 1 kΩ. The system's transmission efficacy has been increased by 35%.

Bao et al. [23] Presented a method for enhancing the coupling k of an inductive connection in a WPT system for implanted devices. The transmitter coil is a spiral shape with a radius of 20 mm, and the receiver coil should be in a solenoid shape with a 0.7 mm wire pitch. The system's coupling k, PTE, and maximum power delivered to the load (MPDL) are determined via simulation and experimentation. Various mediums such as air, muscle, and bone are being tried to evaluate their impact on the gearbox and reception coils. In the muscle (bone) medium, the PTE is 44.14% and 43.07%, while the MPDL is 145.38 mW and 128.13 mW, respectively.

Abed et al. [24] Offered an innovative mathematical and theoretical analysis to enhance the efficiency of the inductive coupling connection. It is achieved using efficient Class-E amplifiers with high and optimal input impedance at 13.56 MHz frequency. The resistance of the implanted device ranges from 200 Ω to 500 Ω with increments of 50 Ω. Power amplifiers exhibit an efficiency of 45% with a load resistance of 50 Ω. This efficiency rises to 49% when the load is adjusted to 41.89 Ω with a coupling coefficient of 0.087. Ouacha et al. [25] Used a new method to enhance a wireless energy transfer system by using the differential evolution algorithm (DEA) to increase PTE and power delivered to the load (PDL). The suggested approach was verified by comparing results with existing methods, achieving a 95% PTE and delivering power with 136 mW to the load at a 130 mm distance. The metaheuristic method enhanced WPT's critical parameters, resulting in a 95% PTE and 136 mW of power to the load.

The research question is that is it possible to reduce the size of the implanted coils receiver while enhancing the efficacy of transfer? This research aims to decrease the dimensions of the implanted coils (receiver) while enhancing the efficacy of transfer. However, the current research showed even better efficiency by using a double-layer technique and reducing the implanted coil size to 8 mm. This approach is a crucial advancement in implantable medical applications since it improves patient comfort using an implanted device.

This study describes a wireless power transmission system for implanted biomedical devices using a Tx-double Rx spiral coil and a single-layer Tx-Rx spiral coil. The receiver's outer diameter is 8.5 mm, whereas the transmitter's is 27 mm. Printed on an FR4 substrate, the system achieves a coupling distance of 2-40 mm in the ISM band at a frequency of 13.56 MHz and tests the proposed design with different loads. The results of this research are significant and novel as it proposes an inductive coupling-double layer square spiral coils (IC-DLSSC) WPT system for implantable medical devices with high efficiency and a small size that uses the 13.56 MHz ISM band frequency. The proposed model is compared with several recent works, demonstrating the effectiveness of the suggested coils in terms of their frequency, transfer distance, higher efficiency, and test SAR.

2. Materials and Methods

This part introduces and examines the inductive coupling technique based on WPT, the theoretical model of the IC-DLSSC WPT coil, the analytical models of IC-DLSSC WPT, and the simulation implemented using HFSS software.

2.1. IC-DLC WPT-based inductive coupling method

Figure 1 shows that the WPT technique comprises three primary components: the primary coil (transmitter circuit Tx), the secondary coil (receiver circuit Rx), and the load. The IC-DLSSC-WPT approach is the most popular and desirable procedure. Transmitter coils are typically positioned on the exterior of the human body, while receiver coils are positioned internally.

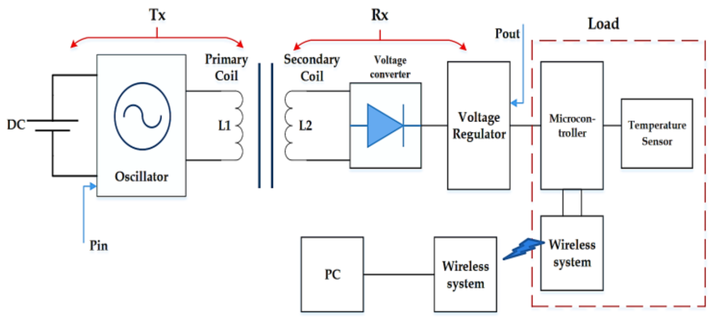

Fig. 1. Simplified IC-DLSSC-WPT system.

2.2. IC-DLC theoretical model

The implementation of a particular coil serves three purposes: inductance (L), series parasitic resistance (Rs), and parallel parasitic capacitance (Cp). The parameters being considered are impacted by many geometric elements, such as the number of turns (n), track width (w), track spacing (s), the inner diameter (Din), and the outer diameter ($d$out) of the copper [26]. The square coil is described by mathematical models in the following manner.

The self-inductance of a square coil can be calculated using Eq. (1) [27]:

$$L = \frac{1.27\mu n^2 d_{avg}}{2}[\ln\frac{2.07}{\varphi} + 0.18\varphi + 0.13\varphi^2] \quad (1)$$

where μ is the permeability of free space (4π x H/m) and conductor, φ is the fill factor, n number of coil turns, d_{avg} is the average diameter of the inductor, and as in these Eqs. (2)-(4):

$$n = \frac{D_{out}\varphi}{(s+w)(1+\varphi)} \quad (2)$$

$$D_{out} = D_{in} + (2n + 1)w + (2n - 1)s \quad (3)$$

$$d_{avg} = \frac{(D_{in}+D_{out})}{2} \quad \text{and} \quad \varphi = \frac{(D_{out}-D_{in})}{(D_{out}+D_{in})} \quad (4)$$

The precision of this expression deteriorates as the ratio of s/w increases significantly, specifically when φ is less than 0.1 or n is less than or equal to 2. It should be noted that the conventional integrated spiral inductor is constructed with a width (s) that is less than or equal to the spacing (w). Spacing between components primarily mitigates the adverse effects of interwinding parasitic capacitance.

Given that the conductor (copper) length of a double-layer spiral coil is equal to double the length of a single PSC layer, it becomes simpler to calculate the series parasitic resistance as shown in Eq. (5).

$$R_s = \frac{2R_{dc}t_c}{\delta(1-e^{-\frac{t_c}{\delta}})} \quad (5)$$

$$\delta = \sqrt{\frac{\rho_c}{\pi\mu f}} \quad \text{and} \quad \mu = \mu_o\mu_r \quad (6)$$

where $R_{dc} = \frac{\rho l_c}{\omega t_c}$ is the resistance of the conductor in direct current (dc), δ is the skin depth, μ_o is the free space's permeability, μ_r is the metal layer's relative permeability, and f is the operating frequency.

In the double-layer coil, parasitic capacitance is present between conductor lines in the upper and lower layers of spiral coils. The substrate functions as a dielectric, as shown in Fig. 2(a). The calculation of parasitic capacitance is performed as in Eq. (7) [28]:

$$C_{p-L} = \frac{\varepsilon_{FR4}\varepsilon_o l_c w}{t_s} \quad (7)$$

where l_c represents the length of copper within each layer and t_s denotes substrate thickness. Therefore, the total parasitic capacitance of the double-layer spiral coil is determined by Eq. (8) [29].

$$C_p = \frac{C_{p-I}}{2} + C_{p-L} \tag{8}$$

The parasitic capacitance ($Cp{-}I$) calculation in single layer spiral coil can be performed using Eq. (9). As depicted in Fig. 2(a).

$$C_{p-I} = \frac{(\alpha\varepsilon_r + \beta\varepsilon_{FR4})\varepsilon_o t_s l_g}{s} \tag{9}$$

$$l_g = 4\, d_{avg}(n-1) \tag{10}$$

The relative dielectric constants of the air and FR4 material are denoted as ε_r and ε_{FR4}, respectively. The value of α = 0.9 and β = 0.1. The gap length (lg) estimation can be derived from (10), indicating a relatively shorter distance than the conductive line's length. The total inductance of a double-layer coil, as depicted in Fig. 2(b), can be expressed as Eq. (11) [30].

$$L_d = L_{s1} + L_{s2} \pm 2M_s \tag{11}$$

The variables L_1 and L_2 represent the inductance value of the first layer and second layer. Additionally, Ms denotes the mutual between the two layers. In the case of a double-layer coil with identical spirals, the self-inductance of each layer can be denoted as $L_1 = L_2 = L_s$. Consequently, the mutual coupling between the two layers can be expressed as Eq. (12).

$$Ms = k_s\sqrt{L_1 L_2} \tag{12}$$

The variable k_s represents the coupling factor that characterizes the link between spiral coils in layers 1 and 2. Considering the structure's additive mutual coupling effect, the cumulative inductance of the two-layer spiral coils is determined.

The coupling between the transmitter and receiver coil can be calculated by using Eq. (13) [31] as shown below:

$$M = k_c\sqrt{L_1 L_2} \tag{13}$$

where k_c is the coupling factor,

$$k_c = \frac{N^2}{0.64[(0.184X^3 - 0.525X^2 + 1.038X + 1.001)(1.67N^2 - 5.84N + 65)]},$$

where, N is the number of coils turns, and X is the distance between the layers in millimetres.

2.3. IC-DLC analytical models

The IC-DLSSC-WPT Analytical system, with the geometrical parameters of the coil in Table 1, has been modelled using the ANSYS Electromagnetics Suite 2022 R1 simulator software. By using Z-parameters, which can easily estimate the electrical parameters of the coils, which include inductances of implanted (receiver) and transmitter coils, (coupling and mutual between the coils (k and M), the quality factor (Q1 and Q2) of coils, series resistance of coils (Rs1 and Rs2) and maximum transfer efficiency (η_{max}), these parameters can be calculated according to the following Eqs. (14)-(19):

$$L_1 = \frac{im(Z(1,1))}{2\pi f} \text{ and } L_2 = \frac{im(Z(2,2))}{2\pi f} \tag{14}$$

$$Q_1 = \frac{im(Z(1,1))}{re(Z(1,1))} \text{ and } Q_2 = \frac{im(Z(2,2))}{re(Z(2,2))} \tag{15}$$

$$k = \sqrt{\frac{im(Z(1,2)) * im(Z(2,1))}{\left(im(Z(2,2)) * im(Z(1,1))\right)}} \tag{16}$$

$$Rs_1 = re(Z(1,1)) \text{ , } Rs_2 = re(Z(2,2)) \tag{17}$$

$$M = \frac{im(Z(2,1))}{2\pi f} \tag{18}$$

$$\eta_{max} = \frac{k^2 Q_1 Q_2}{\left(1+\sqrt{1+k^2 Q_1 Q_2}\right)^2} \tag{19}$$

The Z11, Z12, Z21, and Z22 correspond to the impedance values and interconnections between the coil ports. Z-parameters are vital in various aspects, including impedance matching, network analysis, design optimization, simulation, and modelling. These devices assist in determining the most suitable impedance of design to improve the transfer efficiency.

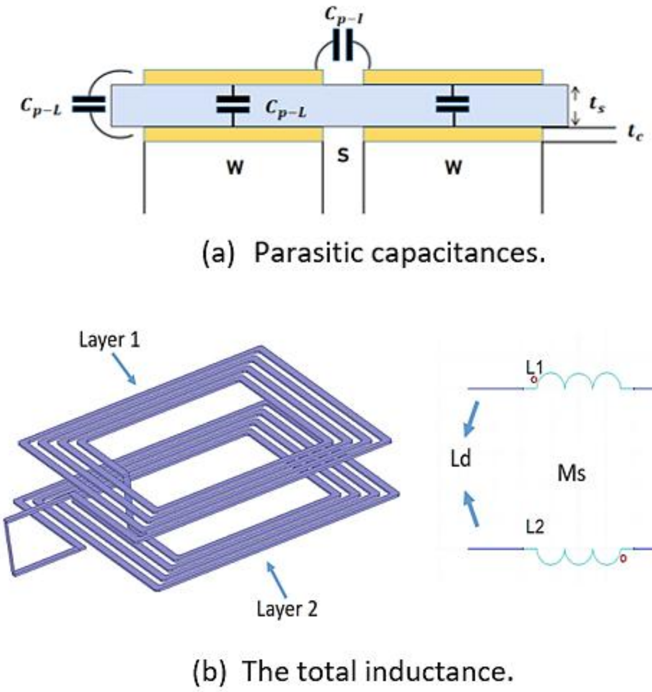

Fig. 2. Double-layer IC-DLSSC (a) Parasitic capacitances, and (b) The total inductance.

2.4. Simulation of IC-DLSSC system for implantable medical device

2.4.1. Single layer design

The suggested system includes a single-layer transmitter and receiver, as Fig. 3(a) illustrates. The key aspects of the design are included in Table 1. The resonance frequency of the design was implemented at 13.56 MHz. The system works in an inductive coupling configuration with a 27 mm outer diameter for the transmitter coil and 8.5 mm for the receiver coil. The system was tested with an air gap (distance) of 10 mm, separating the transmitter and receiver coils. The L1, L2, and M can be calculated using Eq. (14) and (18). Equation (16) measures the coupling coefficient of the receiver coil, and Eq. (19) calculates power transfer efficiency.

Table 1. Single and double coil systems parameters.

Parameters	TX	RX-single	RX-double
Outer diameter, D_{out} (mm)	27	8.5	8.5
Inner diameter, D_{in} (mm)	7	6.5	6.5
Number of coils turns, n (turns)	13	3	3 (for each coil)
Track width, w (mm)	0.55	0.25	0.25
s (mm)	0.25	0.25	0.25
Operating frequency, f	13.56 MHz		
Distance between coils (mm)	2-40		
Conductor thickness (copper) t_c (mm)	0.07		
Substrate thickness t_s (mm)	t_{s1}=1, t_{s2}=0.5		
Substrate dielectric constant (FR4) ϵ_{rFR4}	4.4		
Outer diameter D_{out} (mm)	13.56 MHz		
Inner diameter D_{in} (mm)	2-40		

2.4.2. Double layer design

This research aimed to achieve valid wireless charging of an implanted device, such as a cardiac pacemaker, by obtaining suitable power transfer a double-layer coil was used within an acceptable transfer distance, as shown in Fig. 3(b), The utilization of a double-layer spiral coil demonstrates a notable increase in inductance, coupling coefficient, and quality factor. A double-layer configuration augments conductor width, thereby reducing series resistance. This reduction in resistance subsequently leads to an increase in the quality factor of coils. The parameters and geometries of the resulting double-layer spiral coils are presented in Table 1.

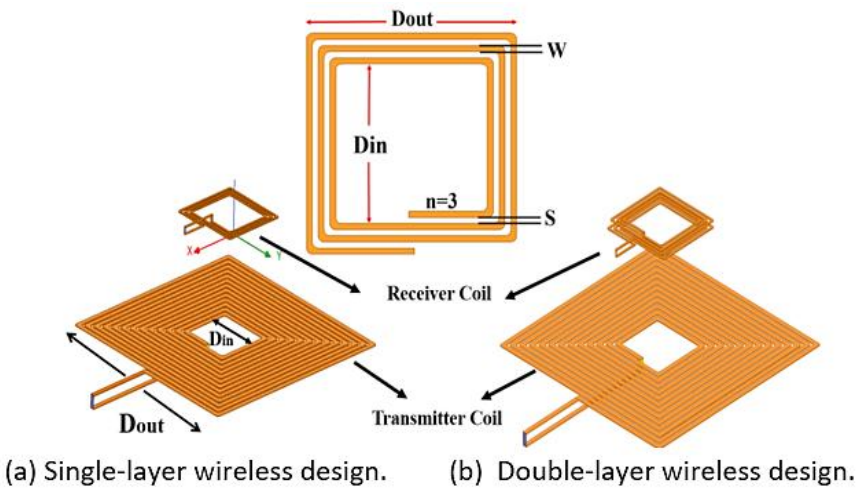

Fig. 3. IC-DLSSC system. (a) Single-layer wireless design, and (b) Double-layer wireless design.

2.5. IC-DLSSC experimental setup

The transmitter and receiver coils are fabricated using the Printed Circuit Board (PCB) technique, as shown in Fig. 4. The FR4 (flame-resistant) substrates used to construct the two coils, which are made of glass fabric and flame-resistant epoxy resin, were chosen due to their low water absorption, strong adherence to copper foil, effective thermal insulation, and exceptional mechanical strength, thickness of 1 mm for the transmitter and 0.5 mm for the receiver. The IC-DLSSC system design coils utilized copper, a high electrical and thermal conductivity material, for signal transmission efficiency and low power loss. They have a track width of 0.55 mm and 0.25 mm for transmitter and receiver coils, respectively, and t_c of 0.07 mm. The receiver coil was fabricated with a double layer printed on the top and bottom of the FR4 substrate, as shown in Fig. 4(c) and (d).

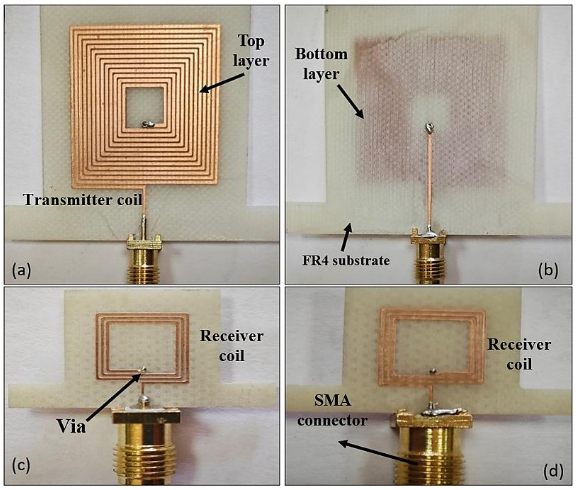

Fig. 4. The fabricated PCB coils (a) and (b) single-layer transmitter coil, top and bottom view, respectively, and (c) and (d) double-layer receiver coil, top and bottom view, respectively.

The test occurred in the Ministry of Science and Technology, Department of Industrial Research and Development, Electronic Manufacturing Centre. The transmitter coil and receiver coil are fixed at a 10 mm distance to examine the validation IC-DLSSC system design, as shown in Figs. 5(a)-(c). Z-parameters with two ports of the inductive coupling model are measured using a vector-network analyser (VNA); the ports of the VNA are linked to the transmitter and receiver coils of the IC-DLSSC system design, respectively.

Because of this, it is easy to extract the coils' electrical parameters. The mutual inductance can be directly obtained by measuring the Z21 parameter. Measures the Z21 parameter by connecting L1 to port one and L2 to port 2 of VNA, as shown in Fig. 5(a). The impedance of port 1 and port 2, which are connected to VNA, was 50 Ω. The measured mutual between the coils using VNA is 43.6 nH, while the simulated value was 78.2 nH. The test in Fig. 5(a) determined the coupling ratio between the transmitting and receiving coils and how much the mutual between the two coils. A high mutual inductance indicated strong coupling between the coils for applications requiring efficient energy transmission.

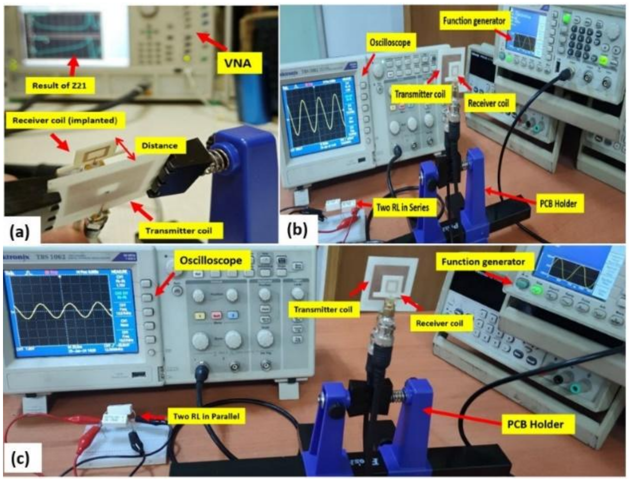

**Fig. 5. Measurement of (a) the test system with a vector network analyser.
(b) the overall system with a load resistor of 300 Ω.
(c) the overall system with a load resistor of 100 Ω.**

3. Results and Discussion

3.1. IC-DLSSC simulation result

This section used the ANSYS Electromagnetic Suite 2022 R1 software program to simulate and build the coils for testing. These coils meet the geometric requirements listed in Table 1. It is possible to determine the k and η values of the inductive coupling by simulating the coils and estimating their electric characteristics. Table 2 presents the acquired electrical characteristics, including the measured Z-parameters, for both the single-layer and double-layer receivers. According to Eq. (14), L1 and L2 are 2.84 µH and 0.40 µH, respectively, at 13.56 MHz. These values indicate that when the size of the coil designed was large, the value of L increased and vice versa.

Table 2. The electrical parameters of design @10 mm distance.

Parameters	Single layer design			Double layer design		
	Modelling Calculation	Simulation Results	Measured Results	Modelling Calculation	Simulation Results	Measured Results
L1 (µH)	2.79	2.83		2.80	2.84	3.182
Q1	74.12	71.96		73.03	70.47	48.65
R_{s1}(Ω)	3.39	3.35		3.48	3.43	5.57
L2(µH)	0.126	0.12	Not Tested	0.41	0.40	0.422
Q2	70.02	68.78		85.04	84.06	60.9
R_{s2}(Ω)	0.149	0.14		0.46	0.40	1.165
k	0.072	0.070		0.073	0.070	0.068
M (nH)	43.4	40.7		79.44	78.2	43.6
η_{max} (%)	67.7	65.29		72.09	70.38	59

Equation (19) was used to calculate the highest power transfer efficiency. The IC-DLSSC design simulations were conducted at various transmission distances. The L1, L2, Rs1, and Rs2 values stay almost constant in each case. However, the alteration in question directly impacts the mutual inductance due to its dependence on Z21, as stated in Eq. (18). The model's coupling coefficient k of the model may be determined by Eq. (16).

Figure 6 displays the highest level of effectiveness achieved by the IC-DLSSC design while operating at a frequency of 13.56 μHz. The transmission distances simulated ranged from 2 to 40 mm. The suggested WPT technology can accurately calculate the highest power transmission efficiency over a wide range of distances. The mutual inductance (M) between the two inductors (L1 and L2) is 78.2 nH when separated by a 10 mm distance. The system initially exhibits a power transfer efficiency of 90.46%, decreasing to 2.56% when the distance between the components ranges from 2 to 40 mm. The double-layer design demonstrates a greater power transfer efficiency value than the single-layer design, with an improved percentage of 7.5%. Furthermore, this research can potentially be applied to cardiac pacemakers.

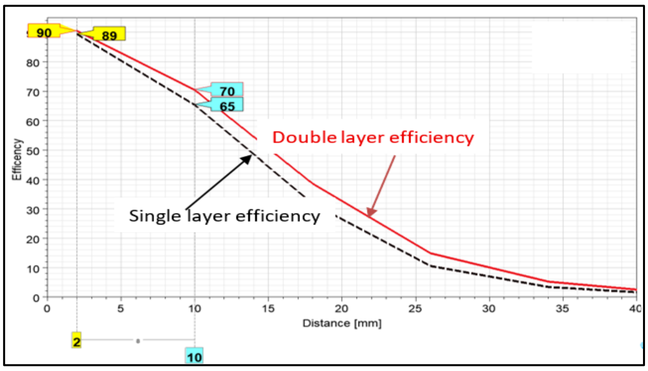

Fig. 6. Power transfer efficiency for single and double layers ranging from 2-40 mm.

3.2. IC-DLSSC experimental results

The load resistance is added to the receiver coil, and the resultant output voltage is computed. This method can be used to determine the power transfer efficiency. A load with values of 75 Ω and 300 Ω was applied to the receiver coil, according to Fig. 5(b) and (c). The efficiency of the measurement result was 59%, while the simulated value was 70.3% when the load resistance was 50 Ω, as shown in Table 2 and Fig. 7. The change in the efficiency between the measurement and simulation values may be attributed to the precision and quality of the manufacturing technologies used. Figure 7 illustrates the comparative efficiency of wireless power transfer for simulated and measured results. Both approaches show a decrease in efficiency as the distance increases, with the difference being stronger at shorter distances.

Figure 8 displays the outcome of the load with different values. The efficiency enhanced as the load resistance value rises. Nevertheless, when the load was 100 Ω and 300 Ω, the efficiency was 27.2% and 47.6%, respectively. Then, when using a 500 Ω load, the efficiency increases to 56%. In Fig. 8, efficiency drops as the distance increases, while higher distances often result in increased losses or decreased performance. Increasing the load resistance leads to improved efficiency at the same distance, indicating that the system functions more effectively with greater resistance loads. On the other hand, lower resistances may be suitable for applications that involve shorter distances. To enhance system efficiency, the researcher should consider both the distance and load resistance. The objective of this test was to evaluate the system's performance when connected to a real load, replicating real-life situations.

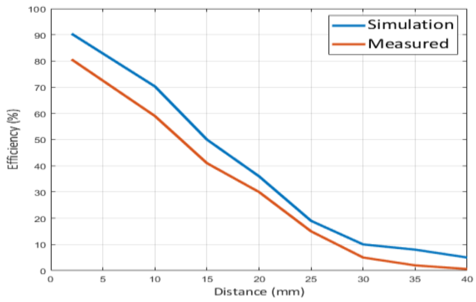

Fig. 7. Efficiency vs. distance for simulated and measured designs at 2 to 40 mm distances.

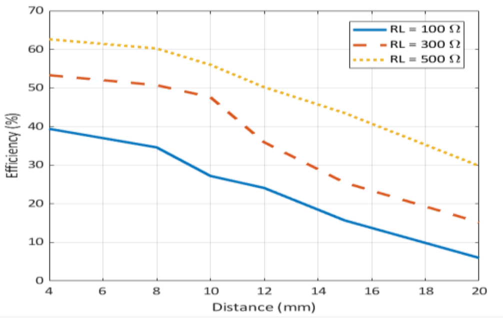

Fig. 8. Efficiency vs. distance with different loads.

3.3. SAR validation

The first step in obtaining the SAR measurements was to project the dimensions of the implanted coil. After that, the SAR is tested on man's head. Figure 9 displays the average SAR distributions at 10 grams of SAR and 1 gram of SAR in W/kg, with 13.56 MHz frequency and 1 W input power. From Fig. 9, the maximum SAR values recorded in the measurement were 0.069 W/kg for a 1 g and 0.0152 W/kg for a 10 g, As shown in the preceding section, the SAR values obtained under the experimental settings are significantly below the SAR levels specified by the US and European standards for 10 g and 1 g of tissue.

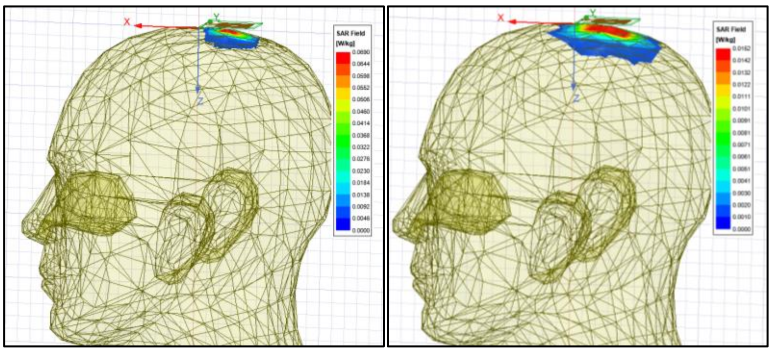

Fig. 9. SAR field measurements on head phantom for (a) 1 gram of SAR and (b) 10 grams of SAR.

4. Comparison with Previous Works

As shown in Table 3, the IC-DLSSC WPT system's implementation was compared with recent related studies regarding frequency, the shape of the coil, transfer distance, transmitter and receiver outer dimensions, efficiency, and SAR test. A comparison was performed to analyse the proposed model against the related design model and establish improved areas. The ISM band frequency used for the IC-DLSSC test was in the same range as that of related studies. The coil configuration impacts design factors, including mutual inductance coupling and efficiency. Transfer distance was an important factor when the coil was designed.

The recommended IC-WPT concept reduces the transmitter's outer diameter and the implanted (receiver) outer diameter. The model is less complex and easier to integrate into various implanted biomedical devices and sensors. Efficiency measures power delivered from the transmitter to the implanted receiver. The SAR test is essential for high-frequency system design. Compared to prior studies, the IC-DLSSC WPT model was more efficient. Increased efficiency sends more power from the transmitter to the implanted receiver coils, making the concept more practical.

To conclude, the IC-DLSSC model performed well across all Table 3 parameters. Its 8.5-mm implanted coil and 59% transmission efficiency at 10 mm made it more compact, and these outcomes were better than previous ones. The findings suggest that the approach might advance wireless power transfer (WPT) for biological applications.

Table 3. IC-DLSSC system model comparison with current investigations.

Ref.	Frequency (MHz)	Shape of coil	Transfer distance (mm)	Transmitter outer diameter (mm)	Receiver outer diameter (mm)	Efficiency (%)	SAR test
Ahire et al. [32]	6.78	square	10	55	35	85.51	-
Xu et al. [22]	13.56	circular	6	20	20	35	> 2 W/kg
Gong et al. [33]	2	circular	8	40	20	59	> 2 W/kg
Omran et al. [34]	13.56	square	4	28	8	44.2	-
Luo et al. [21]	13.56	square	10	40	10	70	-
Ha-Van and Seo [35]	13.56	Square-helical	50-80	100	9	-	> 2 W/kg
Proposed design	13.56	square	10	27	8.5	59	> 2 W/kg

5. Conclusions

This work suggests wirelessly delivering energy to biomedical implanted devices using double-layer inductive coupling. IC-DLSSC has a 13.56 MHz frequency and an 8.5 mm implanted coil. For design, ANSYS Electromagnetics Suite 2022 simulated the IC-DLSSC WPT system. Tested models examined how distance and load affect power transmission efficiency. The double-layer design outperforms the single-layer variant by 7.5%. The IC-DLSSC design performed well in SAR measurements. This concept may be used cardiac pacemaker to monitor vital signs and diagnose ailments, improving patient quality of life. Efficiency decreases dramatically when the transmitter circuit and receiver distance rise. In WPT system design and implementation, distance-dependent behaviour requires careful coil selection to achieve performance at different operating distances. Future research should examine other topics to improve the proposed system. Coil shape optimization, alignment, biomedical equipment integration, and real-world testing and validation are covered.

Nomenclatures

C_p	parasitic capacitance
d_{avg}	Average diameter of the inductor
D_{out}	Outer diameter
D_{in}	Inner diameter

Greek Symbols

μ	Permeability of free space.
δ	Skin depth
μ_o	Free space permeability
μ_r	Metal layer relative permeability
ε_r	Relative dielectric constants of the air

Abbreviations

DSO	Digital storage oscilloscope
FCC	Federal Communications Commission
HFSS	High-Frequency Simulator Structure
IC-DLSSC	Inductive coupling-double layer square spiral coil
ISM	Industrial, Scientific, and Medical
PCBs	Printed circuit boards
PTE	Power Transfer Efficiency
WPT	Wireless power transfer

References

1. Alemaryeen, A.; and Noghanian, S. (2023). A survey of the thermal analysis of implanted antennas for wireless biomedical devices. *Micromachines*, 14(10), 1894.
2. Omer, A.E.; Safavi-Naeini, S.; Hughson, R.; and Shaker, G. (2020). Blood glucose level monitoring using an FMCW millimeter-wave radar sensor. *Remote Sensing*, 12(3), 385.
3. Galetsi, P.; Katsaliaki, K.; and Kumar, S. (2023). Exploring benefits and ethical challenges in the rise of mHealth technology for the common good: An analysis of mobile applications for health specialists. *Technovation*, 121, 102598.
4. Migdał, P.; Murawska, A.; Bieńkowski, P.; Berbeć, E.; and Roman, A. (2021). Changes in honeybee behaviour parameters under the influence of the E-field at 50 Hz and variable intensity. *Animals*, 11(2), 247.
5. Singer, A.; and Robinson, J.T. (2021). Wireless power delivery techniques for miniature implantable bioelectronics. *Advanced Healthcare Materials*, 10(17), 2100664.

6. Mahmood, A.I.; Gharghan, S.K.; Eldosoky, M.A.; and Soliman, A.M. (2022). Near-field wireless power transfer used in biomedical implants: A comprehensive review. *IET Power Electronics*, 15(16), 1936-1955.
7. Van Mulders, J.; Delabie, D.; Lecluyse, C.; Buyle, C.; Callebaut, G.; Van der Perre, L.; and De Strycker, L. (2022). Wireless power transfer: Systems, circuits, standards, and use cases. *Sensors*, 22(15), 5573.
8. Mahmood, A.I.; Gharghan, S.K.; Eldosoky, M.A.; and Soliman, A.M. (2023). Wireless charging for cardiac pacemakers based on class-D power amplifier and a series-parallel spider-web coil. *International Journal of Circuit Theory and Applications*, 51(1), 1-17.
9. Ahire, D.B.; Gond, V.J.; and Chopade, J.J. (2022). Compensation topologies for wireless power transmission system in medical implant applications: A review. *Biosensors and Bioelectronics*: *X*, 11, 100180.
10. Zhang, J.; Das, R.; Zhao, J.; Mirzai, N.; Mercer, J.; and Heidari, H. (2022). Battery-free and wireless technologies for cardiovascular implantable medical devices. *Advanced Materials Technologies*, 7(6), 2101086.
11. Pietrelli, L.; Ferro, S.; and Vocciante, M. (2019). Eco-friendly and cost-effective strategies for metals recovery from printed circuit boards. *Renewable and Sustainable Energy Reviews*, 112, 317-323.
12. Chakraborty, M.; Kettle, J.; and Dahiya, R. (2022). Electronic waste reduction through devices and printed circuit boards designed for circularity. *IEEE Journal on Flexible Electronics*, 1(1), 4-23.
13. Espera Jr., A.H.; Dizon, J.R.C.; Chen, Q.; and Advincula, R.C. (2019). 3D-printing and advanced manufacturing for electronics. *Progress in Additive Manufacturing*, 4(3), 245-267.
14. Cao, L.; Liu, Y.; Zhang, Y.; Cao, Y.; Li, J.; Chen, J.; Zhang, L.; and Qi, Z. (2022). Thermal conductivity and bending strength of SiC composites reinforced by pitch-based carbon fibres. *Journal of Advanced Ceramics*, 11(2), 247-262.
15. Zhang, Y.; Liu, W.; Li, N.; Qian, Z.; Wang, B.; Liu, D.; and Li, X. (2021). Design of a new type of omnidirectional shear-horizontal EMAT using half-ring magnets and PCB technology. *Ultrasonics*, 115, 106465.
16. Ferreira, D.; Caldeirinha, R.F.S.; Cuinas, I.; and Fernandes, T.R. (2018). A review of manufacturing materials and production methods for frequency-selective structures. *IEEE Antennas and Propagation Magazine*, 60(6), 110-119.
17. Wang, Y.; Xu, C.; Yu, X.; Zhang, H.; and Han, M. (2022). Multilayer flexible electronics: Manufacturing approaches and applications. *Materials Today Physics*, 23, 100647.
18. Buga, C.S.; and Viana, J.C. (2021). A review on materials and technologies for organic large-area electronics. *Advanced Materials Technologies*, 6(6), 2001016.
19. Ribeiro, P.P.M.; Santos, I.D.; and Dutra, A.J.B. (2019). Copper and metals concentration from printed circuit boards using a zig-zag classifier. *Journal of Materials Research and Technology*, 8(1), 513-520.
20. Min, H.-G.; Kang, D.-J.; and Park, J.-H. (2020). Comparison of tensile and fatigue properties of copper thin film depending on process method. *Applied Sciences*, 10(1), 388.

21. Luo, J.; Xue, R.; Cheong, J.; Zhang, X.; and Yao, L. (2023). Design and optimization of planar spiral coils for powering implantable neural recording microsystem. *Micromachines*, 14(6), 1221.
22. Xu, D.; Zhang, Q.; and Li, X. (2020). Implantable magnetic resonance wireless power transfer system based on 3D flexible coils. *Sustainability*, 12(10), 4149.
23. Bao, J.; Hu, S.; Xie, Z.; Hu, G.; Lu, Y.; and Zheng, L. (2022). Optimization of the coupling coefficient of the inductive link for wireless power transfer to biomedical implants. *International Journal of Antennas and Propagation*, 2022(1), 8619514.
24. Abed, B.H.; Majeed, J.H.; and Habeeb, N.A. (2021). Optimization of bio-implantable power transmission efficiency based on input impedance. *Computer Systems Science and Engineering*, 38(1), 17-24.
25. Ouacha, B.; Bouyghf, H.; Mohammed, N.; and Abenna, S. (2022). DEA-based optimization of inductive coupling for powering implantable biomedical devices. *International Journal of Power Electronics and Drive Systems*, 13(3), 1558-1567.
26. Du, X.; and Dujic, D. (2023). Modeling and design optimization of loosely coupled PCB spiral coils in inductive power transfer systems. *IEEE Transactions on Power Electronics*, 38(11), 13430-13442.
27. Noroozi, B.; and Morshed, B.I. (2024). Misalignment-tolerant planar spiral coil pair design for 13.56 MHz inductive coupling of wireless resistive analogue passive sensors. *Sensors*, 24(3), 752.
28. Wang, Q.; Saket, M.A.; Troy, A.; and Ordonez, M. (2021). A self-compensated planar coil for resonant wireless power transfer systems. *IEEE Transactions on Power Electronics*, 36(1), 674-682.
29. Wang, X.; Pang, J.; Tan, Q.; Dong, H.; Zhao, N.; and Xue, T. (2021). Design of double-layer parallel printed spiral coil for wireless power transfer applied to rotating equipment. *Sensors and Actuators A*: *Physical*, 331, 112761.
30. Faria, A.; Marques, L.; Ferreira, C.; Alves, F.; and Cabral, J. (2021). A fast and precise tool for multi-layer planar coil self-inductance calculation. *Sensors*, 21(14), 4864.
31. Zhao, J. (2010). A new calculation for designing multilayer planar spiral inductors. *EDN-Electrical Design News*, 55(14), 37.
32. Ahire, D.B.; Gond, V.J.; and Chopade, J.J. (2022). Geometrical parameter optimization of planner square-shaped printed spiral coil for efficient wireless power transfer system to biomedical implant application. *e-Prime-Advances in Electrical Engineering*, *Electronics and Energy*, 2, 100045.
33. Gong, C.; Liu, D.; Miao, Z.; and Li, M. (2017). A magnetic-balanced inductive link for simultaneous uplink data and power telemetry. *Sensors*, 17(8), 1768.
34. Omran, M.M.; Mutashar, S.; and Ezzulddin, A. (2019). Design of an (8×8) mm^2 efficient inductive power link for medical applications. *Proceedings of the* 2*nd* *International Conference on Engineering Technology and its Applications* (*IICETA*), *Al-Najaf, Iraq*, 61-66.
35. Ha-Van, N.; and Seo, C. (2019). Modeling and experimental validation of a butterfly-shaped wireless power transfer in biomedical implants. *IEEE Access*, 7, 107225-107233.